

Dynamic Interference of Photoelectrons Produced by High-Frequency Laser Pulses

Philipp V. Demekhin^{1,2,*} and Lorenz S. Cederbaum^{1,†}

¹*Theoretische Chemie, Physikalisch-Chemisches Institut, Universität Heidelberg, Im Neuenheimer Feld 229, D-69120 Heidelberg, Germany*

²*Rostov State Transport University, Narodnogo Opolcheniya Square 2, Rostov-on-Don, 344038, Russia*
(Received 26 November 2011; published 18 June 2012)

The ionization of an atom by a high-frequency intense laser pulse, where the energy of a single photon is sufficient to ionize the system, is investigated from first principles. It is shown that as a consequence of an ac Stark effect in the continuum, the energy of the photoelectron follows the envelope of the laser pulse. This is demonstrated to result in strong dynamic interference of the photoelectrons of the same kinetic energy emitted at different times. Numerically exact computations on the hydrogen atom demonstrate that the dynamic interference spectacularly modifies the photoionization process and is prominently manifested in the photoelectron spectrum by the appearance of a distinct multipeak pattern. The general theory is well approximated by explicit analytical expressions that allow for a transparent understanding of the discovered phenomena and for making predictions on the dependence of the measured spectrum on the pulse.

DOI: [10.1103/PhysRevLett.108.253001](https://doi.org/10.1103/PhysRevLett.108.253001)

PACS numbers: 33.20.Xx, 41.60.Cr, 82.50.Kx

Dipole transitions between bound electronic states of matter mediated by intense laser pulses are affected by a fundamental energy shift induced by the oscillating external field of the laser known as the dynamic or ac Stark effect [1–8]. The ac Stark effect induced by optical laser fields is used in a myriad of contemporary experiments to hold and align molecules [9], to shape potential energy surfaces [10], to make rapid transient birefringence [11,12], and to control quantum systems [13,14]. What happens if the transition is to the continuum and not to a bound electronic state? Here, we investigate the photoionization of an atom by a high-frequency strong laser pulse, where the energy of a single photon is sufficient to ionize the system. We demonstrate that the interplay between the photoionization and the ac Stark shift results in a hitherto unrecognized dynamic interference of photoelectrons of the same kinetic energy emitted at different times. The effect is universal and prominently manifested in the photoelectron spectrum.

In bound-bound electronic transitions accessible to optical lasers, the ac Stark effect detunes the laser frequency away from the field-free resonant frequency, an effect that has to be compensated for in the presence of strong fields in order to have a transition. The situation is different in the case of ionization. The new generation of light sources, like the free electron laser (FEL) at FLASH [15], and recent progress in high-order harmonic generation techniques [16,17] allow one to produce ultrashort laser pulses with single-photon energies well above the ionization threshold of any matter. This immediately raises the fundamental question of how the well-studied, single-photon ionization process in weak fields will be modified in intense laser fields of high frequencies. We shall demonstrate here that single-photon ionization by high-frequency strong pulses is accompanied by dynamic interference caused by the ac Stark effect in the continuum.

In order to illustrate the new fundamental effect, we have chosen as an explicit example the photoionization of the hydrogen atom which is not affected by many-electron correlations and, thus, is amenable to exact computations. The ac Stark effect arises from the indirect coupling of nonresonant (nonessential) states that do not participate directly in the excitation process [18]. To arrive at an unequivocal description of the process, we have computed exactly the quantum motion of the whole discrete and continuum electron spectrum of hydrogen exposed to a strong pulse. For the sake of transparency of presentation, we show below explicitly only the essential states (i.e., $1s \rightarrow \varepsilon p$ ionization) and employ the simplifying rotating wave approximation (RWA), which turns out to describe well the underlying physics. In the full calculations, we have used also the nonessential states and discarded the RWA (see below and Appendix for details).

An atom initially in its ground electronic state $|I\rangle$ of energy of $E_I = 0$ (chosen as the origin of the energy scale) is ionized into the final electron continuum state $|F\varepsilon\rangle$ of energy $IP + \varepsilon$ (where $IP = E_F - E_I$ is the ionization potential and ε is the kinetic energy of the photoelectron) by a linearly polarized laser pulse of carrier frequency ω and pulse-shape function $g(t)$. Following [19–24], the total wave function of the system as a function of time reads

$$\Psi(t) = a_I(t)|I\rangle + \int d\varepsilon a_\varepsilon(t)|F\varepsilon\rangle e^{-i\omega t}, \quad (1)$$

where $a_I(t)$ and $a_\varepsilon(t)$ are the time-dependent amplitudes of the populations of the initial and final continuum states, the latter being dressed by the field (redefined by multiplying with the phase factor $e^{i\omega t}$ [21]). Inserting $\Psi(t)$ into the time-dependent Schrödinger equation for the total Hamiltonian of the atom plus its interaction with the laser

field, we obtain the following set of equations for the amplitudes (atomic units are used throughout)

$$i\dot{a}_I(t) = \int d\varepsilon \left\{ \frac{1}{2} d_\varepsilon^\dagger \mathcal{E}_0 \right\} g(t) a_\varepsilon(t), \quad (2a)$$

$$i\dot{a}_\varepsilon(t) = \left\{ \frac{1}{2} d_\varepsilon \mathcal{E}_0 \right\} g(t) a_I(t) + (IP + \varepsilon - \omega) a_\varepsilon(t). \quad (2b)$$

\mathcal{E}_0 is the peak amplitude of the field $\mathcal{E}(t) = \mathcal{E}_0 g(t) \cos \omega t$, and $d_\varepsilon = \langle F\varepsilon | \hat{z} | I \rangle$ is the energy-dependent ionization dipole transition matrix element, which can be exactly computed for hydrogen.

The calculations were performed for a Gaussian-shaped pulse, $g(t) = e^{-t^2/\tau^2}$, and carrier frequency $\omega = 53.6057$ eV, which is well above the ionization potential $IP = 13.6057$ eV. The photoelectron spectra computed for two pulse durations and different peak intensities (defined as $I = \mathcal{E}_0^2/8\pi\alpha$) are depicted in Fig. 1. One can see that the effect of a strong laser pulse on the spectra is enormous. Instead of a single peak at $\varepsilon_0 = \omega - IP = 40$ eV with the width of the pulse as naively expected from weak-field calculations, the spectra are substantially shifted and spread and possess distinct modulations of the intensity. The effect is so big that it can easily be verified experimentally.

To uncover the underlying physics, we show the time evolution of the photoelectron spectrum in Fig. 2 computed

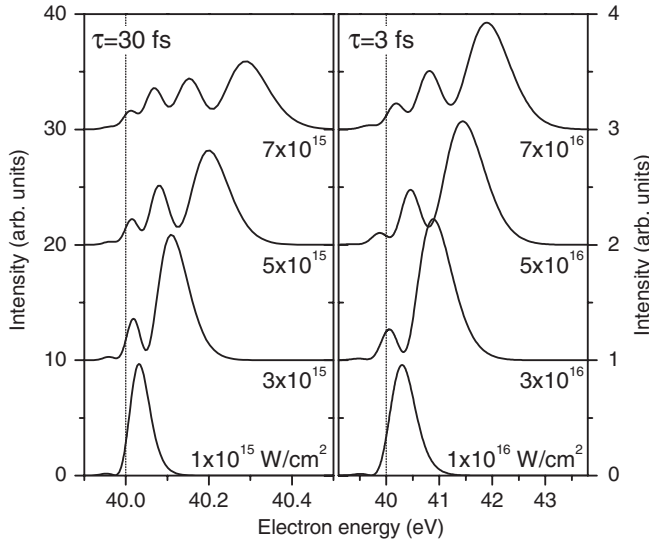


FIG. 1. Photoelectron spectra of the hydrogen atom exposed to Gaussian-shaped pulses of 30 fs (left panel) and 3 fs (right panel) durations with carrier frequency $\omega = 53.6057$ eV computed exactly for different peak intensities. In weak-field single-photon ionization, the photoelectron line appears as a Gaussian peak centered around the energy of $\varepsilon_0 = \omega - IP = 40$ eV (indicated by the vertical broken line) and a width provided by the pulse: FWHM of about 52 meV for the 30 fs pulse, and 0.52 eV for the 3 fs pulse. The presently computed strong pulse ionization spectra are, however, much broader (by several times), shifted to higher energies from the central electron energy of $\varepsilon_0 = 40$ eV, and possess distinct modulations of the electron intensity. It will be shown that these modulations are due to dynamic interference in the continuum.

for the 30 fs pulse and peak intensity of 5×10^{15} W/cm². At short times, the spectrum develops symmetrically around $\varepsilon_0 = 40$ eV as expected for weak fields. Until the maximum of the pulse arrives, the spectrum remains nearly symmetric, but its maximum continuously shifts to higher energies. Importantly, strong modulations of the intensity start to develop in the spectrum only after the maximum of the pulse has passed. This will be explained below.

So far, we discussed the spectra computed exactly. Now, we would like to interpret the findings by introducing approximations that allow us to arrive at explicit analytic expressions and proven to be surprisingly accurate. In the local approximation [25,26], Eq. (2a) reads

$$i\dot{a}_I(t) = \left(\Delta - \frac{i}{2}\Gamma \right) g^2(t) a_I(t). \quad (3)$$

Here, the real term, $\Delta g^2(t)$, is nothing but the ac Stark shift of the energy of the ground state immersed into the dressed continuum. As usual, this shift follows the intensity envelope of the field [18], i.e. $g^2(t)$. Derivations of the expression for Δ can be found, e.g. in [18], and in the present case it explicitly reads (without using the RWA)

$$\Delta = -\mathcal{P} \int d\varepsilon \left| \frac{d_\varepsilon \mathcal{E}_0}{2} \right|^2 \left(\frac{1}{IP + \varepsilon - \omega} + \frac{1}{IP + \varepsilon + \omega} \right), \quad (4)$$

where \mathcal{P} stands for the principal value of the integral. In the RWA approximation, the second term on the rhs of Eq. (4)

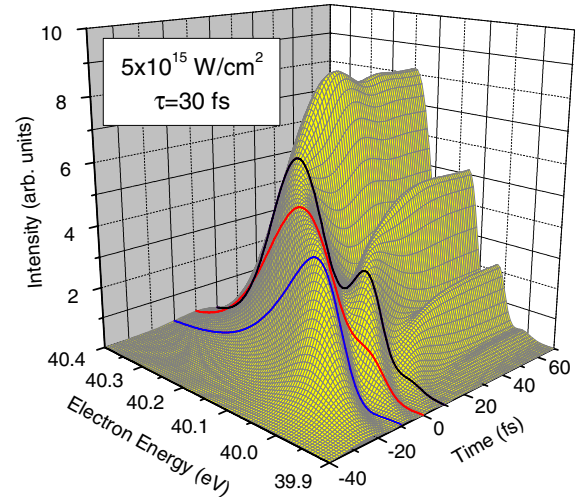


FIG. 2 (color online). Time evolution of the photoelectron spectrum computed exactly for the hydrogen atom exposed to a Gaussian-shaped pulse of 30 fs duration, of carrier frequency $\omega = 53.6057$ eV, and peak intensity of 5×10^{15} W/cm². At very early times, the spectrum starts to develop symmetrically around the central electron energy of $\varepsilon_0 = 40$ eV. At later times, but before the maximum of the pulse arrives, the maximum of the spectrum moves to higher electron energies (see the spectrum computed at -10 fs). When the pulse arrives (the time 0 fs corresponds to the pulse maximum), the spectrum is not any more symmetric but still does not possess intensity modulations. The first modulations start to show up in the spectrum only after the pulse maximum (see the spectrum computed at $+10$ fs) has arrived.

is neglected. The value of Δ is proportional to the peak intensity, $\Delta \sim \mathcal{E}_0^2 \sim I$, and it is essentially nonzero owing to the energy dependence of the dipole matrix element d_ε .

The imaginary term $-\frac{i}{2}\Gamma g^2(t)$ in Eq. (3) describes the losses of the population of the ground state by the ionization into all final electron continuum states $|F\varepsilon\rangle$. Γ can be obtained from Δ in Eq. (4). The explicit expression for Γ was obtained in [21] in the local and RWA approximations and in the present case it reads

$$\Gamma = 2\pi \left| \frac{1}{2} d_{\varepsilon_0} \mathcal{E}_0 \right|^2. \quad (5)$$

Eq. (5) is also valid without using the RWA, since the second term in the energy integral (4) possesses no pole. The decay rate Γ is also responsible for the additional broadening of the photoelectron peaks beyond the width given by the pulse intensity envelope.

Equation (3) can be solved explicitly

$$a_I(t) = e^{(-i\Delta - \Gamma/2)J(t)}, \quad (6)$$

where $J(t) = \int_{-\infty}^t g^2(t') dt'$ grows smoothly with time. We find that the result (6) is in excellent agreement with the exact calculations. It also simplifies greatly the computation of the spectrum. As it stands, $a_\varepsilon(t)$ in Eq. (2b) can be expressed as an integral of $a_I(t)$ [19,21]

$$a_\varepsilon(t) = -i \left[\frac{1}{2} d_\varepsilon \mathcal{E}_0 \right] e^{-i\delta t} \int_{-\infty}^t g(t') a_I(t') e^{i\delta t'} dt', \quad (7)$$

where we introduced the abbreviation $\delta = IP + \varepsilon - \omega = \varepsilon - \varepsilon_0$, which is the electron energy detuning from ε_0 . Using now the explicit expression (6) makes the computations of $a_\varepsilon(t)$ and of the spectrum $\sigma(\varepsilon) = |a_\varepsilon(+\infty)|^2$ rather straightforward.

The photoelectron spectrum computed in the local approximation is depicted in the upper panel of Fig. 3. The ac Stark shift $\Delta = 0.26$ eV and the decay rate $\Gamma = 0.044$ eV computed via the above equations (4) and (5) have been utilized in the numerical calculations. It is seen that the spectrum calculated in the local approximation (solid curve) describes very well the exact spectrum (open circles).

Due to the success of the local approximation, we are able to gain deeper insight into the origin of the interference effects leading to the intensity modulation in the spectrum by evaluating analytically $a_\varepsilon(t)$. For this purpose, we notice that the integrand in Eq. (7) contains a rapidly oscillating factor $\exp[i\delta t' - i\Delta J(t')]$ that is multiplied by a smoothly varying function. The main contributions to the integral stem from the times at which the phase $\Phi(t) = \delta t - \Delta J(t)$ is stationary [27], i.e. $\dot{\Phi} = 0$. The resulting stationary phase condition, $\Delta g^2(t_s) = \delta$, has a transparent physical meaning. It defines the time $t_s(\varepsilon)$ at which the energy of the ground state, continuously shifted by the ac Stark effect, moves across the energy position ε of the dressed continuum state ($\delta = \varepsilon - \varepsilon_0$). For any pulse, there are at least two stationary points for each value of ε : one, $t_1(\varepsilon)$, when the pulse is growing, and another, $t_2(\varepsilon)$, when

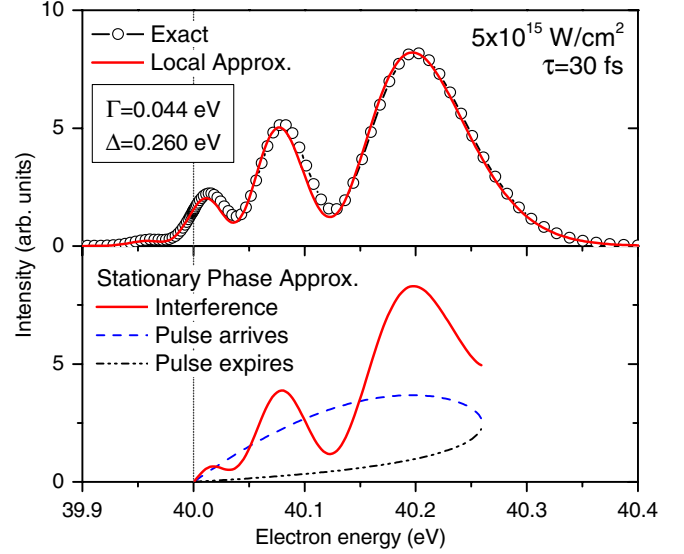


FIG. 3 (color online). Upper panel: The photoelectron spectrum of the hydrogen atom exposed to a Gaussian-shaped pulse of 30 fs duration, carrier frequency $\omega = 53.6057$ eV, and peak intensity 5×10^{15} W/cm² computed exactly (open circles) compared with the spectrum computed in the local approximation (solid curve) with the quantities $\Gamma = 0.044$ eV and $\Delta = 0.26$ eV. Lower panel: The spectrum obtained in the stationary phase approximation via Eq. (8) with the same parameters (solid curve). The two individual contributions to the spectrum from the negative and positive times $t_s = \pm t_1(\varepsilon) = \pm \tau \sqrt{\ln[\Delta/(\varepsilon - \varepsilon_0)]/2}$ describing in Eq. (8) the contributions when the pulse arrives and expires, respectively, are shown by broken curves. The energy-dependent interference term in Eq. (8) is proportional to $\cos\{-2(\varepsilon - \varepsilon_0)t_1 - \Delta[J(-t_1) - J(+t_1)] - \pi/2\}$. In the energy interval $\varepsilon - \varepsilon_0 \in [0, \Delta]$ for which a stationary phase can be found, its argument accumulates a phase of $\Delta J(+\infty)$, which for a Gaussian pulse is equal to $\Delta \tau \sqrt{\pi/2}$. For the present parameters, the interference term accumulates a phase of $14.85 \approx 2.36 \times 2\pi$ rad, and, thus, the spectrum exhibits around two and a half oscillations of the intensity profile as seen in the figure.

it decreases. For a Gaussian pulse there are exactly two times, $t_1(\varepsilon) = -t_2(\varepsilon)$.

By collecting in the integral (7) these two main contributions at $t_s = \pm t_1(\varepsilon)$, we obtain the following explicit approximate expression for the spectrum

$$\sigma(\varepsilon) = \left| \frac{d_\varepsilon \mathcal{E}_0}{2} \sum_{t_s = \pm t_1(\varepsilon)} g(t_s) e^{-\Gamma/2 J(t_s)} e^{i[\Phi(t_s) \pm \pi/4]} \right|^2. \quad (8)$$

The additional phase factors $\pm \frac{\pi}{4}$ result from higher terms in the expansion of the phase $\Phi(t)$ around the stationary points $\pm t_1(\varepsilon)$ computed for the Gaussian pulse. The photoelectron spectrum evaluated via Eq. (8) is depicted in the lower panel of Fig. 3 (solid curve). It is illuminating to see that an explicit simple expression reproduces nicely the exact spectrum (open circles in the upper panel of the figure) which is complicated to compute. The individual contributions to the spectrum of the two terms in the

expression (8) are smooth and rather boring (broken curves in the lower panel of the figure).

Equation (8) allows one to uncover the physical origin of the strong modulations in the photoelectron spectrum. These are the results of the coherent superposition of two photoelectron waves emitted with the same kinetic energy at two different times. A cartoon visualizing this dynamic interference is shown in Fig. 4. This new physical effect causes enormous qualitative changes in the photoelectron spectrum which can easily be verified experimentally. Importantly, the interferences vanish if the ac Stark shift in the continuum vanishes (i.e., if Δ vanishes). Then, there are no stationary points along the pulse. We would like to stress that the dynamic interference can be controlled by the shape of the pulse envelope and is influenced by the choice of the carrier frequency. We are convinced that dynamic interference is a universal effect in ionization processes by high-frequency strong laser pulses and its experimental investigation is feasible. In the following, we address these issues in some detail.

The predicted phenomenon also persists in other systems with more electrons. In the hydrogen atom discussed above, the residual ion does not possess electrons and, therefore, the dynamic interference is governed by the ac

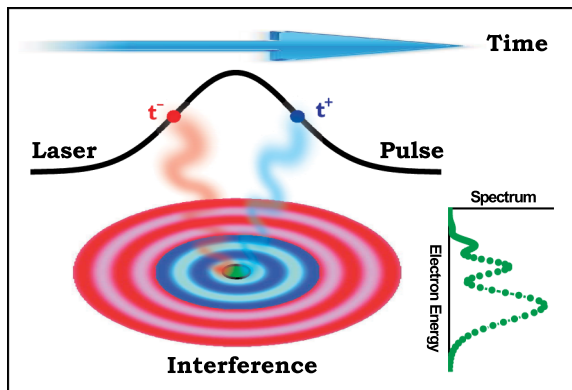


FIG. 4 (color online). The intense laser pulse of sufficient high frequency to ionize the system by one-photon absorption induces a time-dependent ac Stark shift of the ground state of the system. Because of this dynamic shift, the photoelectron emitted along the pulse envelope has at every moment t predominantly a specific kinetic energy ε which is determined by that t (at a given time t , the phase contributing to the integrand in Eq. (7) is stationary at $\varepsilon = \varepsilon_0 + g^2(t)\Delta$, for details see text). Owing to the fact that the pulse envelope first grows and then falls, there are for a Gaussian pulse exactly two times (indicated as t^- and t^+ in the figure) at which the emitted electron wave has the same energy ε . These two waves emitted with a time delay with respect to each other interfere. This dynamic interference gives rise to the strongly modulated intensity distribution of the photoelectron spectrum seen in Figs. 1–3. The dynamic interference can be controlled by the intensity, duration, carrier frequency, and shape of the pulse. A pulse envelope with more than one maximum leads to more than two waves that interfere and higher laser intensity to larger ac Stark shift Δ and to more oscillations of the spectrum.

Stark shift $g^2(t)\Delta$ which is a property of the ground state in the field. If the ion produced by photoionization does possess electrons, then this ion is obviously also subject to an ac Stark shift $g^2(t)\Delta_{\text{Ion}}$. In this case, the dynamic interference pattern in the spectrum is governed by the total ac Stark shift $g^2(t)\Delta_{\text{Tot}}$ where $\Delta_{\text{Tot}} = \Delta - \Delta_{\text{Ion}}$ [28]. As the ion is usually harder to ionize than the neutral system, one can expect that Δ_{Tot} will be substantial even if both Δ and Δ_{Ion} have the same sign. Moreover, depending on the photon energy ω , the shifts Δ and Δ_{Ion} can have different signs, enhancing interference effects (see an explicit example in [28]). In many-electron systems, several electronic shells can be subject to the ionization, and different ionic states can be produced. Each ionic continuum will contribute to the shift of the ground electronic state leading all together to a final unique value of Δ at the carrier frequency ω . In general, different ionic states $|F_\alpha\rangle$ will experience different ac Stark shifts $g^2(t)\Delta_{\text{Ion}}^\alpha$. The dynamic interference pattern in each of the partial electron spectra is determined by different total shifts $\Delta_{\text{Tot}}^\alpha = \Delta - \Delta_{\text{Ion}}^\alpha$ [28], and one can expect dissimilar dynamic interference patterns in different partial photoelectron spectra. Experimental investigations of dynamic interference will be possible, in particular, if the studied ionic thresholds are not too close to each other, i.e., if the resulting partial spectra do not overlap. The ac Stark shift scales also with the probability to ionize the system. As photoionization cross sections usually decrease with the photon energy, the shift will be larger for frequencies ω that are not too far from the ionization threshold. In general, one can expect particularly large shifts, and, hence, more pronounced interference patterns, in systems with cross sections that vary strongly with the photon energy, e.g., in the vicinity of a shape resonance.

To demonstrate the feasibility of experiments on dynamic interference, we discuss the present status of FEL facilities. The currently operating FEL at FLASH [15] generates soft x-ray radiation in the energy range of 26–180 eV with flux of about 10^{13} photons per pulse with durations of 10–70 fs [29]. Combined with appropriate focusing optics, peak irradiance levels of more than 10^{16} W/cm² can be achieved at present [30]. So far, the SASE FEL sources do not produce monochromatic radiation, and their pulses consist of many spikes with randomly fluctuating properties. The impact of these problems on the experimental output has been studied, e.g., in Ref. [31]. Nevertheless, the pulse properties at FLASH are continuously improving, and an average temporal coherence of 3–6 fs can already be achieved [32]. Moreover, several new techniques have been proposed for improvement [33], such as the selection of a single ultrashort radiation spike [34]. In addition, the recently tested FEL facility FERMI at Elettra [35] operates in single-mode, providing coherent pulses (without spikes) with durations of 30 to 100 fs in the photon energy range of 12 to 413 eV, and it is expected to provide an unprecedented flux of about 10^{14} photons per pulse. Concluding, the

pulse durations, photon energies, temporal coherence, and peak intensities necessary for experiments on dynamic interference are available at present.

In conclusion, intense high-frequency pulses give rise to a strong ac Stark effect in the continuum, which, in turn, modifies the ionization process dramatically. The effects are universal and can be verified experimentally by current techniques. Whenever matter is exposed to intense pulses, like in FEL experiments, ionization takes place, and the ac Stark effects in the continuum and the resulting dynamic interference will come into play. They will be essential for understanding the experimental results. The effects are thus both fundamental for light-matter interaction and of practical importance for the analysis of FEL experiments.

We thank A. I. Kuleff for many valuable discussions.

APPENDIX.—In this Appendix, we discuss how the full calculations were done. We have numerically solved exactly the system of equations that accounts for the interaction of all essential and nonessential electronic states of hydrogen with the laser pulse without employing the rotating wave approximation. For the peak intensities considered here, the effect essentially stems from the quantum motion of the electron eigenstates restricted to ns and nd Rydbergs with $n \leq 6$, mp Rydbergs with $m \leq 16$, and, of course, εp continuum with $\varepsilon \leq 100$ eV. Let us designate the time-dependent amplitudes for the population of the even ns/nd states by $a_e(t)$, and for the odd $mp/\varepsilon p$ states by $a_o(t)$. The system of equations of motion of these states in the presence of the pulse reads

$$\begin{aligned} i\dot{a}_e(t) &= E_e a_e(t) + \sum_{\text{odd}} \left(\frac{\mathcal{E}_0}{2} (d_e^o)^\dagger \right) g(t) (e^{i\omega t} + e^{-i\omega t}) a_o(t) \\ i\dot{a}_o(t) &= E_o a_o(t) + \sum_{\text{even}} \left(\frac{\mathcal{E}_0}{2} d_e^e \right) g(t) (e^{i\omega t} + e^{-i\omega t}) a_e(t) \end{aligned} \quad (\text{A1})$$

with boundary conditions $a_{1s}(-\infty) = 1$ and $a_{i \neq 1s}(-\infty) = 0$ for all other amplitudes. The continuous spectrum was discretized as $|F\varepsilon\rangle = |F\varepsilon_k\rangle \cdot \sqrt{\Delta\varepsilon_k}$, where $|F\varepsilon_k\rangle$ represents the state in the continuum interval of $\Delta\varepsilon_k$ centered around the electron energy ε_k . The energy steps $\Delta\varepsilon_k$ were chosen linear with respect to $\sqrt{\varepsilon}$ and concentrated symmetrically around the central electron energy ε_0 . The convergence of the solution with respect to the electron eigenstates included, of the integration over time and of the discrete representation of the continuous energy, has been ensured.

*philipp.demekhin@pci.uni-heidelberg.de

†lorenz.cederbaum@pci.uni-heidelberg.de

- [1] M. V. Fedorov, *Atomic and Free Electrons in a Strong Light Field* (World Scientific, Singapore, 1997).
[2] L. Allen and J. H. Eberly, *Optical Resonance and Two-Level Atoms* (Dover, Minneola, 1987).

- [3] C. Gerry and P. Knight, *Introductory Quantum Optics* (Cambridge University Press, Cambridge, 2004).
[4] R. Loudon, *The Quantum Theory of Light* (Oxford University Press, Oxford, 2000), 3rd ed..
[5] N. B. Delone and V. P. Krainov, *Phys. Usp.* **42**, 669 (1999).
[6] W. Happer, *Prog. Quantum Electron.* **1**, 51 (1970).
[7] S. H. Autler and C. H. Townes, *Phys. Rev.* **100**, 703 (1955).
[8] M. Haas, U. D. Jentschura, and C. H. Keitel, *Am. J. Phys.* **74**, 77 (2006).
[9] H. Stapelfeldt and T. Seideman, *Rev. Mod. Phys.* **75**, 543 (2003).
[10] B. J. Sussman, D. Townsend, M. Yu. Ivanov, and A. Stolow, *Science* **314**, 278 (2006).
[11] P. J. Bustard, B. J. Sussman, and I. A. Walmsley, *Phys. Rev. Lett.* **104**, 193902 (2010).
[12] A. V. Sokolov and S. E. Harris, *J. Opt. B: Quantum Semiclassical Opt.* **5**, R1 (2003).
[13] S. A. Rice and M. Zhao, *Optical Control of Molecular Dynamics* (Wiley, New York, 2000).
[14] P. W. Brumer and M. Shapiro, *Principles of the Quantum Control of Molecular Processes* (Wiley, New York, 2003).
[15] W. Ackermann *et al.*, *Nat. Photon.* **1**, 336 (2007).
[16] G. Sansone *et al.*, *Science* **314**, 443 (2006).
[17] E. Goulielmakis *et al.*, *Science* **320**, 1614 (2008).
[18] B. J. Sussman, *Am. J. Phys.* **79**, 477 (2011).
[19] E. Pahl, H.-D. Meyer, and L. S. Cederbaum, *Z. Phys. D* **38**, 215 (1996).
[20] Y.-C. Chiang, P. V. Demekhin, A. I. Kuleff, S. Scheit, and L. S. Cederbaum, *Phys. Rev. A* **81**, 032511 (2010).
[21] Ph. V. Demekhin and L. S. Cederbaum, *Phys. Rev. A* **83**, 023422 (2011).
[22] L. S. Cederbaum, Y.-C. Chiang, P. V. Demekhin, and N. Moiseyev, *Phys. Rev. Lett.* **106**, 123001 (2011).
[23] P. V. Demekhin, Y.-C. Chiang, and L. S. Cederbaum, *Phys. Rev. A* **84**, 033417 (2011).
[24] P. V. Demekhin, S. D. Stoychev, A. I. Kuleff, and L. S. Cederbaum, *Phys. Rev. Lett.* **107**, 273002 (2011).
[25] L. S. Cederbaum and W. Domcke, *J. Phys. B* **14**, 4665 (1981).
[26] W. Domcke, *Phys. Rep.* **208**, 97 (1991).
[27] N. Bleistein and R. Handelsman, *Asymptotic Expansions of Integrals*. (Dover, New York, 1975).
[28] See Supplemental Material at <http://link.aps.org/supplemental/10.1103/PhysRevLett.108.253001> for more details on the theory.
[29] K. Tiedtke *et al.*, *New J. Phys.* **11**, 023029 (2009).
[30] A. A. Sorokin, S. V. Bobashev, T. Feigl, K. Tiedtke, H. Wabnitz, and M. Richter, *Phys. Rev. Lett.* **99**, 213002 (2007).
[31] N. Rohringer and R. Santra, *Phys. Rev. A* **77**, 053404 (2008).
[32] S. Roling, B. Siemer, M. Wöstmann, H. Zacharias, R. Mitzner, A. Singer, K. Tiedtke, and I. A. Vartanyants, *Phys. Rev. ST Accel. Beams* **14**, 080701 (2011).
[33] J. Feldhaus, J. Arthur, and J. B. Hastings, *J. Phys. B* **38**, S799 (2005).
[34] E. L. Saldin, E. A. Schneidmiller, and M. V. Yurkov, *Opt. Commun.* **212**, 377 (2002).
[35] Home page of Free Electron Laser for Multidisciplinary Investigations FERMI at Elettra in Trieste, Italy, <http://www.elettra.trieste.it/FERMI/>.